

Non-linear radiation influence on oblique stagnation point flow of Maxwell fluid

A. Ghaffari^{a,*}, T. Javed^b, and I. Mustafa^c

^a*Department of Mathematics, University of Education,
Attock Campus, Attock 43600, Pakistan.*

* Tel.: +923325505532

e-mail: abuzar.ghaffari@ue.edu.pk

^b*Department of Mathematics and Statistics, FBAS, International Islamic University,
Islamabad 44000, Pakistan.*

^c*Department of Mathematics, Allama Iqbal Open University,
H-8, Islamabad 44000, Pakistan.*

Received 22 September 2017; accepted 23 January 2018

Non-linear thermal radiation effects on non-aligned stagnation point flow of Maxwell fluid have been carried out in the present investigation. It is observed that the non-linear radiation augments the temperature and heat transfer rate. This physical phenomenon is translated into a system of partial differential equations (PDEs). After useful transformation, these non-linear constitutive equations are transformed into a system of ordinary differential equations (ODEs) and interpreted numerically by means of parallel shooting technique. Effects of pertinent parameters on flow and heat transfer are elaborated through tables and graphs. It is observed that radiation and surface heating enhance the rate of heat transfer, however Prandtl number has inverse relation with thermal boundary layer thickness. It has been observed that for increasing Prandtl number, heat transfer rate enhances. The detailed discussion of heat transfer rate is also presented in this study. Flow pattern is judged through streamlines graphs. It is also observed that oblique stagnation point flow behaves like orthogonal stagnation point flow, when free stream velocity is very large as compared to stretching velocity.

Keywords: Maxwell fluid; oblique stagnation point; thermal radiation; parallel shooting method.

PACS: 47.10.ad; 47.15.Cb; 44.40.+a; 44.20.+b

1. Introduction

A stagnation-point arises when fluid strikes at a surface and, its velocity becomes zero. During the last few decades, stagnation point flows have been studied by many researchers. The interest of researchers in stagnation point flow is due to its wide applications in industrial and engineering problems, such as cooling of nuclear reactors and electronic devices by fans, solar central receivers exposed to wind currents [1-3], the environment [4] and several others. The maximum heat transfer and pressure gradient are observed in the region of the stagnation point flow. Figure 1 shows that the fluid strikes at a stretching surface with an arbitrary angle of incidence, and the fluid away from the surface moves with the free stream velocity $U_e = ax + by$ (x and y are coordinates along x -axis and y -axis respectively and a and b are dimensional constants having dimension $[1/T]$). Stuart [5] was the first who initiated the work in this field and found analytical solution for the case when fluid impinging obliquely at the plane surface. Tamada [6], and Dorrepaal [7], generalized the case of stagnation point. In their study, they found the solution of oblique stagnation point flow (when the fluid is making acute angle with the plate). However, at right angle the case of orthogonal stagnation point flow can also be achieved. Oblique stagnation flow over a stretching surface was initially investigated by Reza and Gupta [8]. They found that no boundary layer exists when stretching and free stream velocities become same. Husain *et al.* [9] extended the work

of oblique stagnation point flow for viscoelastic fluid model, Mahapatra *et al.* [10] studied radiation effects in oblique stagnation point region, Lok *et al.* [11], considered micropolar fluid model and Yajun *et al.* [12] studied magnetic effects on heat and fluid flow in stagnation point region.

Unlike Newtonian fluid model, which are governed by a single constitutive equation, non-Newtonian fluid models are complex and it is hard to express them in a single constitutive equation. Different types of models have been proposed by many researchers due to their applications in industries. Amongst these models, the Maxwell model has received a special attention due to its simplicity describing the rheological effects of viscoelastic fluids. Wang and Tan [13], used modified Maxwell model to study the linear stability with sores effects. They found that oscillatory convection of system destabilized by the sores effect and instability of the system increases with the increase of relaxation time. Noor Fadiya [14] studied the hydromagnetic flow of Maxwell fluid under thermophoretic effects and found Homotopic solutions and analyzed that the boundary layer thickness is decreasing function of thermophoretic parameter. Javed and Ghaffari [15], generalized the idea of stagnation point flow of Maxwell fluid. Abel *et al.* [16], Mukhopadhyay [17], Nadeem *et al.* [18] also carried out further studies.

Flow over a stretching surface has significant importance due to its extensive use in industries such as wire drawing, hot rolling, cooling of metallic sheets, glass fibers, and many others. Magyari and Keller [19] widely discussed this topic

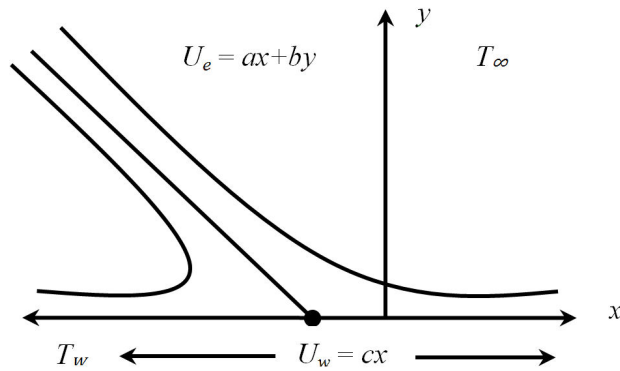


FIGURE 1. Sketch of the physical plane considered in this study.

theoretically and numerically. During the last few decades, the study of stagnation point flow over a stretching surface has remained an interesting problem for many researchers. Crane [20] was the first, who studied the stretching sheet problem and found analytical solution. Rajagopal *et al.* [21] was among the earlier scientists who studied the flow of a viscoelastic fluid over a stretching sheet, Mahapatra and Gupta [22] discussed magnetic effects in the region of the stagnation point flow over a stretching sheet. Nazar *et al.* [23] investigated a micropolar fluid flow over a stretching sheet in the stagnation point region. Later, Layek *et al.* [24], Hayat *et al.* [25], Zhu *et al.* [26], and Bhattacharyya [27] discussed various effects of the stagnation point flow on linear and non-linear stretching surface.

During the technological processes at high temperatures (e.g. cooling glass sheet etc.), thermal radiation effects play an important role which cannot be neglected. Gupta and Gupta [28] studied the heat transfer over a stretching surface with suction or blowing and discussed the different aspects of the problem. Recently, Mahapatra and Gupta [29] investigated heat transfer in stagnation point region toward a stretching sheet. Raptis *et al.* [30] studied the effects of thermal radiation on hydromagnetic flow. Pop *et al.* [31] extended the work of Mahapatra and Gupta by introducing radiation effects. In present problem study of oblique stagnation point flow of Maxwell fluid with radiation effects over a stretching sheet has been carried out numerically using parallel shooting technique. Effects of different parameter on heat and fluid flow are discussed through tables and graphs. in detail. An excellent agreement of results has been found with Pop *et al.* [31] and Labropulu *et al.* [32].

2. Flow equations

In present study, steady two-dimensional oblique stagnation point flow of Maxwell fluid over a stretching sheet is considered. The stretching sheet is taken along the plane $y = 0$ and flow is confined along y -axis. The sheet is stretched with velocity $U_w = cx$, where $c (> 0)$ is stretching constant. The governing equations of the present problem are

$$\text{div} \bar{\mathbf{V}} = 0, \tag{1}$$

$$\rho \frac{d\bar{\mathbf{V}}}{dt} = -\nabla p + \text{div} \bar{\mathbf{S}}, \tag{2}$$

$$\bar{u} \frac{\partial \bar{T}}{\partial \bar{x}} + \bar{v} \frac{\partial \bar{T}}{\partial \bar{y}} = \frac{k}{\rho c_p} \bar{\nabla}^2 \bar{T} - \frac{1}{\rho c_p} \bar{\nabla} \cdot \bar{q}_r, \tag{3}$$

Where “div” represents divergence operator, $\bar{\mathbf{V}} = [\bar{u}, \bar{v}, 0]$ is the velocity vector, \bar{u} and \bar{v} are velocity components along \bar{x} and \bar{y} coordinates. Where bar represents the dimensional quantities, later these quantities will be converted into dimensionless form. p is the pressure, ρ is the density, k is the thermal conductivity of the fluid, c_p is the specific heat at constant pressure \bar{T} and represents the temperature of the fluid. The radiative heat flux \bar{q}_r and extra stress tensor $\bar{\mathbf{S}}$ for Maxwell fluid are defined as

$$\bar{q}_r = -\frac{4\sigma^*}{3(\alpha_r + \sigma_s)} \frac{\partial \bar{T}^4}{\partial \bar{y}}, \tag{4}$$

$$\bar{\mathbf{S}} + \bar{\lambda}_1 \frac{D\bar{\mathbf{S}}}{Dt} = \mu \bar{\mathbf{A}}_1, \tag{5}$$

where σ^* , α_r , α_s , μ , and λ_1 are the Stefan-Boltzmann constant, the Rosseland mean absorption coefficient, the scattering coefficient, dynamic viscosity of the fluid, and relaxation time of the material respectively. $\bar{\mathbf{A}}_1$ is the first Rivlin-Ericksen tensor defined by

$$\bar{\mathbf{A}}_1 = \bar{\mathbf{L}} + \bar{\mathbf{L}}^T, \tag{6}$$

where $\bar{\mathbf{L}}$ is the velocity gradient and $\bar{\mathbf{L}}^T$ represents its transpose defined as

$$\bar{\mathbf{L}} = \begin{bmatrix} \frac{\partial \bar{u}}{\partial \bar{x}} & \frac{\partial \bar{u}}{\partial \bar{y}} & 0 \\ \frac{\partial \bar{v}}{\partial \bar{x}} & \frac{\partial \bar{v}}{\partial \bar{y}} & 0 \\ 0 & 0 & 0 \end{bmatrix} \text{ and } \bar{\mathbf{L}}^T = \begin{bmatrix} \frac{\partial \bar{u}}{\partial \bar{x}} & \frac{\partial \bar{v}}{\partial \bar{x}} & 0 \\ \frac{\partial \bar{u}}{\partial \bar{y}} & \frac{\partial \bar{v}}{\partial \bar{y}} & 0 \\ 0 & 0 & 0 \end{bmatrix}$$

The operator D/Dt is defined for a contravariant vector and for a contravariant tensor of rank 2 respectively in Eq. (7) and (8) as suggested in Ref. 33

$$\frac{D\bar{\mathbf{S}}}{Dt} = \frac{d\bar{\mathbf{S}}}{dt} - \bar{\mathbf{L}}\bar{\mathbf{S}}, \tag{7}$$

$$\frac{D\bar{\mathbf{S}}}{Dt} = \frac{d\bar{\mathbf{S}}}{dt} - \bar{\mathbf{L}}\bar{\mathbf{S}} - \bar{\mathbf{S}}\bar{\mathbf{L}}^T. \tag{8}$$

Applying divergence on both sides of Eq. (5), we get

$$\left(1 - \lambda_1 \frac{D}{Dt}\right) \nabla \cdot \bar{\mathbf{S}} = \mu \nabla \cdot \bar{\mathbf{A}}_1, \tag{9}$$

operating $(1 + \lambda_1(D/Dt))$ on both side of Eq. (2) and then eliminating $(1 + \lambda_1(D/Dt)) \nabla \cdot \bar{\mathbf{S}}$ from Eq. (9), we obtain

$$\left(1 - \lambda_1 \frac{D}{Dt}\right) \left(\rho \frac{d\bar{\mathbf{V}}}{dt} + \nabla p\right) = \mu \nabla \cdot \bar{\mathbf{A}}_1. \tag{10}$$

The second factor on left side of the above equation is a vector, using Eqs. (7) and (1), Eq. (10) takes the following form in components

x-component:

$$\begin{aligned} \bar{u} \frac{\partial \bar{u}}{\partial \bar{x}} + \bar{v} \frac{\partial \bar{u}}{\partial \bar{y}} = & -\frac{1}{\rho} \frac{\partial p}{\partial \bar{x}} - \frac{\lambda_1}{\rho} \left(\bar{u} \frac{\partial^2 p}{\partial \bar{x}^2} + \bar{v} \frac{\partial^2 p}{\partial \bar{x} \partial \bar{y}} \right. \\ & \left. - \frac{\partial \bar{u}}{\partial \bar{x}} \frac{\partial p}{\partial \bar{x}} - \frac{\partial \bar{u}}{\partial \bar{y}} \frac{\partial p}{\partial \bar{y}} \right) + \mathbf{v} \left(\frac{\partial^2 \bar{u}}{\partial \bar{x}^2} + \frac{\partial^2 \bar{u}}{\partial \bar{y}^2} \right) \\ & - \lambda_1 \left(\bar{v}^2 \frac{\partial^2 \bar{u}}{\partial \bar{y}^2} + 2\bar{u}\bar{v} \frac{\partial^2 \bar{u}}{\partial \bar{x} \partial \bar{y}} + \bar{u}^2 \frac{\partial^2 \bar{u}}{\partial \bar{x}^2} \right), \end{aligned} \quad (11)$$

y-component:

$$\begin{aligned} \bar{u} \frac{\partial \bar{v}}{\partial \bar{x}} + \bar{v} \frac{\partial \bar{v}}{\partial \bar{y}} = & -\frac{1}{\rho} \frac{\partial p}{\partial \bar{y}} - \frac{\lambda_1}{\rho} \left(\bar{v} \frac{\partial^2 p}{\partial \bar{y}^2} + \bar{u} \frac{\partial^2 p}{\partial \bar{x} \partial \bar{y}} \right. \\ & \left. - \frac{\partial \bar{v}}{\partial \bar{x}} \frac{\partial p}{\partial \bar{x}} - \frac{\partial \bar{v}}{\partial \bar{y}} \frac{\partial p}{\partial \bar{y}} \right) + \mathbf{v} \left(\frac{\partial^2 \bar{v}}{\partial \bar{x}^2} + \frac{\partial^2 \bar{v}}{\partial \bar{y}^2} \right) \\ & - \lambda_1 \left(\bar{v}^2 \frac{\partial^2 \bar{v}}{\partial \bar{y}^2} + 2\bar{u}\bar{v} \frac{\partial^2 \bar{v}}{\partial \bar{x} \partial \bar{y}} + \bar{u}^2 \frac{\partial^2 \bar{v}}{\partial \bar{x}^2} \right), \end{aligned} \quad (12)$$

The boundary conditions of the current flow problem are [29]

$$\begin{aligned} \bar{u} = c\bar{x}, \quad \bar{v} = 0 \quad \text{at} \quad \bar{y} = 0, \\ \bar{u} = a\bar{x} + b\bar{y}, \quad \text{as} \quad \bar{y} \rightarrow \infty, \end{aligned} \quad (13)$$

where *a*, *b* and *c* are positive constants having dimension (time)⁻¹. By using boundary layer approximation [31], the above equations reduce to the following form

$$\begin{aligned} \bar{u} \frac{\partial \bar{u}}{\partial \bar{x}} + \bar{v} \frac{\partial \bar{u}}{\partial \bar{y}} = & -\frac{1}{\rho} \frac{\partial p}{\partial \bar{x}} - \frac{\lambda_1}{\rho} \left(-\frac{\partial \bar{u}}{\partial \bar{y}} \frac{\partial p}{\partial \bar{y}} \right) + \mathbf{v} \frac{\partial^2 \bar{u}}{\partial \bar{y}^2} \\ & - \lambda_1 \left(\bar{v}^2 \frac{\partial^2 \bar{u}}{\partial \bar{y}^2} + 2\bar{u}\bar{v} \frac{\partial^2 \bar{u}}{\partial \bar{x} \partial \bar{y}} + \bar{u}^2 \frac{\partial^2 \bar{u}}{\partial \bar{x}^2} \right), \end{aligned} \quad (14)$$

Introducing the following transformation as suggested by Labropulu *et al.* [29]

$$\begin{aligned} x = \bar{x} \sqrt{\frac{c}{v}}, \quad y = \bar{y} \sqrt{\frac{c}{v}}, \quad u = \frac{1}{\sqrt{vc}} \bar{u}, \\ v = \frac{1}{\sqrt{vc}} \bar{v}, \quad P = \frac{1}{\rho vc} p, \end{aligned} \quad (15)$$

We obtain the following equation in dimensionless form

$$\begin{aligned} u \frac{\partial u}{\partial x} + v \frac{\partial u}{\partial y} = & -\frac{\partial p}{\partial x} + \lambda_1 c \left(-\frac{\partial u}{\partial y} \frac{\partial p}{\partial y} \right) + \mathbf{v} \frac{\partial^2 u}{\partial y^2} \\ & - \lambda_1 c \left(v^2 \frac{\partial^2 u}{\partial y^2} + 2uv \frac{\partial^2 u}{\partial x \partial y} + u^2 \frac{\partial^2 u}{\partial x^2} \right), \end{aligned} \quad (16)$$

and boundary conditions take the form as

$$\begin{aligned} u = x, \quad v = 0 \quad \text{at} \quad y = 0, \\ u = \frac{a}{c}x + \frac{b}{c}y, \quad \text{as} \quad y \rightarrow \infty \end{aligned} \quad (17)$$

Let us assume that ambient temperature of the fluid is *T*_∞ and the temperature of the stretching plate is *T*_w. The energy equation in dimensionless form using the transformation given in Eq. (15) reduces to the following form

$$\begin{aligned} u \frac{\partial T}{\partial x} + v \frac{\partial T}{\partial y} = & \frac{1}{Pr} \frac{\partial}{\partial y} \left(\left(1 \right. \right. \\ & \left. \left. + \frac{4}{3} Rd(1 + (\theta_w - 1)T)^3 \right) \frac{\partial T}{\partial y} \right), \end{aligned} \quad (18)$$

and boundary conditions are

$$T(0) = 1, \quad T(\infty) = 0, \quad (19)$$

where Pr is the Prandtl number, *θ*_w is the surface temperature, and Rd is the radiation parameter defined as:

$$Pr = \frac{\mu c_p}{k}, \quad \theta_w = \frac{T_w}{T_\infty}, \quad Rd = \frac{4\sigma * T_\infty^3}{k(\alpha_r + \sigma_s)}. \quad (20)$$

By using the continuity equation, we define the stream function *ψ* such that

$$u = \frac{\partial \psi}{\partial y}, \quad v = -\frac{\partial \psi}{\partial x} \quad (21)$$

Now substituting Eq. (21) in Eqs. (16-19)

$$\begin{aligned} \frac{\partial \psi}{\partial y} \left(\frac{\partial^2 \psi}{\partial x \partial y} \right) - \frac{\partial \psi}{\partial x} \left(\frac{\partial^2 \psi}{\partial y^2} \right) + \beta \left(\left(\frac{\partial \psi}{\partial x \partial y} \right)^2 \frac{\partial^3 \psi}{\partial y^3} \right. \\ \left. - 2 \frac{\partial \psi}{\partial y} \frac{\partial \psi}{\partial x} \frac{\partial^3 \psi}{\partial x \partial y} + \left(\frac{\partial \psi}{\partial y} \right)^2 \frac{\partial^3 \psi}{\partial x^2 \partial y} \right) \\ = -\frac{\partial P}{\partial x} + \beta \frac{\partial^2 \psi}{\partial y^2} \frac{\partial P}{\partial y} + \frac{\partial^3 \psi}{\partial y^3} \end{aligned} \quad (22)$$

$$\begin{aligned} \frac{\partial \psi}{\partial y} \frac{\partial T}{\partial x} - \frac{\partial \psi}{\partial x} \frac{\partial T}{\partial y} = & \frac{1}{Pr} \frac{\partial}{\partial y} \left(\left(1 + \frac{4}{3} \right. \right. \\ & \left. \left. \times Rd(1 + (\theta_w - 1)T)^3 \right) \frac{\partial T}{\partial y} \right), \end{aligned} \quad (23)$$

$$y = 0 : \quad \psi = 0, \quad \frac{\partial \psi}{\partial y} = x, \quad T = 1$$

$$y \rightarrow \infty : \quad \psi = \frac{a}{c}xy + \frac{1}{2}\gamma y^2, \quad T = 0, \quad (24)$$

where *β* = *λ*₁*c* is a dimensionless number called Deborah number, which represents the fluidity of the material and *γ* = *b/c* represents the shear in the free stream. Suppose that the solution of Eqs. (22,23) subjected to the boundary conditions defined in Eq. (24) is of the form

$$\psi = xf(y) + g(y), \quad T = \theta(y), \quad (25)$$

where the functions *f*(*y*) and *g*(*y*) are normal and oblique component of the flows. Using the Eq. (25) in Eqs. (22-24),

we get

$$\begin{aligned} & f'(y)(xf'(y) + g'(y)) - f(y)(xf''(y) + g''(y)) \\ & + \beta((f(y))^2(xf'''(y) + g'''(y)) \\ & - 2f(y)f''(y)(xf'(y) + g'(y))) \\ & = -\frac{\partial P}{\partial x} + \beta(xf''(y) + g''(y))\frac{\partial P}{\partial y} \\ & + xf'''(y) + g'''(y), \end{aligned} \tag{26}$$

$$\begin{aligned} & \frac{\partial}{\partial y} \left[\left\{ 1 + \frac{4}{3}Rd(1 + (\theta_w - 1)\theta)^3 \right\} \theta' \right] \\ & + Prf\theta' = 0, \end{aligned} \tag{27}$$

$$\begin{aligned} y = 0 : \quad & f(y) = 0, \quad f'(y) = 1, \\ g(y) = g'(y) = 0, \quad & \theta = 1 \\ y \rightarrow \infty : \quad & f'(y) = \frac{a}{c}, \quad g'(y) = \gamma y, \quad \theta = 0. \end{aligned} \tag{28}$$

After eliminating the pressure, Eq. (26) takes the form as

$$\begin{aligned} & f'(y)(xf'(y) + g'(y)) - f(y)(xf''(y) + g''(y)) \\ & + \beta((f(y))^2(xf'''(y) + g'''(y)) \\ & - 2f(y)f''(y)(xf'(y) + g'(y))) \\ & = x \left(\frac{a}{c} \right)^2 - A\gamma + xf'''(y) + g'''(y), \end{aligned} \tag{29}$$

where A is a constant that accounts the boundary layer displacement. After comparing the coefficients of x^1 and x^0 in Eq. (29), following system of equations is obtained

$$f''' + ff'' - (f')^2 + \left(\frac{a}{c} \right)^2 + \beta(2ff'f'' - f^2f''') = 0 \tag{30}$$

$$g''' + fg'' - f'g' + \beta(2ff''g' - f^2g''') = A\gamma, \tag{31}$$

Energy equation is

$$\frac{\partial}{\partial y} \left[\left\{ 1 + \frac{4}{3}Rd(1 + (\theta_w - 1)\theta)^3 \right\} \theta' \right] + Prf\theta' = 0 \tag{32}$$

and boundary conditions are

$$\begin{aligned} y = 0 : \quad & f(y) = 0, \quad f'(y) = 1, \\ g(y) = g'(y) = 0, \quad & \theta(y) = 1, \\ y \rightarrow \infty : \quad & f'(y) = \frac{a}{c}, \\ g'(y) = \gamma y, \quad & \theta(y) = 0. \end{aligned} \tag{33}$$

Where the prime denotes the derivative with respect to y . For the simplicity, a new variable is introduced which is defined as $g'(y) = \gamma h(y)$, Eq. (31) with boundary conditions reduce to

$$h'' + fh' - f'h + \beta(2ff''h - f^2h'') = A, \tag{34}$$

$$h(0) = 0h'(\infty) = 1. \tag{35}$$

It is necessary to mentioned here that for a Newtonian fluid ($\beta = 0$) and orthogonal stagnation point flow ($\gamma = 0$) Eqs. (30) and (32) reduce to Eqs. (6) and (7) as reported by Pop *et al.* [31]. The dimensionless components of velocity are

$$\begin{aligned} u &= \frac{\partial \psi}{\partial y} = xf'(y) + g'(y), \\ v &= -\frac{\partial \psi}{\partial x} = -f(y). \end{aligned} \tag{36}$$

The physical quantity of interest is the local Nusselt number, which is defined as

$$\begin{aligned} Nu_x &= \frac{\bar{x}q_w}{k(T_w - T_\infty)} \quad \text{and} \\ q_w &= -\left[\left(\frac{16\sigma\bar{T}^3}{3(\alpha_r + \sigma_s)} + k \right) \frac{\partial \bar{T}}{\partial \bar{y}} \right] \end{aligned} \tag{37}$$

Upon using dimensionless variables given in Eq. (15) the above equation reduces to

$$Nu_x(Re_x)^{-1/2} = -\left(1 + \frac{4}{3}Rd\theta_w^3 \right) \theta'(0). \tag{38}$$

3. Numerical method

Non-linear equations (30), (32), and (34) subject to the boundary conditions (33) and (35) have been solved numerically by using parallel shooting method [34]. For the solution of highly non-linear problems, the parallel shooting method is better as compared to the simple shooting method because the simple shooting method is hard to use due to its dependence on initial guess. The method of parallel shooting is very efficient for the solution of this kind of problems. The method is described as follows

- (i) Equations (30), (32) and (34), are reduced in the system of first order differential equations by letting $f = f_1, h = f_4$ and $\theta = f_6$

$$\left. \begin{aligned} f'_1 &= f_2, \quad f'_2 = f_3, \\ f'_3 &= \frac{1}{1-\beta f_1^2} (-f_1f_3 + f_2^2 - 2\beta f_1f_2f_3 - \left(\frac{a}{c}\right)^2) \\ f'_4 &= f_5, \\ f'_5 &= \frac{1}{1-\beta f_1^2} (-f_1f_5 + f_2f_4 - 2\beta f_1f_3f_4 + A) \\ f'_6 &= f_7, \\ f'_7 &= \left(1 + \frac{4}{3}Rd(1 + (\theta_w - 1)f_6)^3 \right)^{-1} \\ &\quad \times ((-4Rd(\theta_w - 1)(1 + (\theta_w - 1)f_6)^2)(f_7)^2 - Prf_1f_7) \end{aligned} \right\}$$

and boundary conditions are expressed as

$$\begin{aligned} f_1(0) = 0, \quad f_2(0) = 1, \quad f_2(y_\infty) &= \frac{a}{c}, \\ f_4(0) = 0, \quad f_5(y_\infty) &= 1, \\ f_6(0) = 1, \quad f_6(y_\infty) &= 0 \end{aligned}$$

TABLE I. The Numerical values of $f''(0)$, $h'(0)$ and A for the different values a/c , for Newtonian fluid ($\beta = 0$).

| a/c | $f''(0)$ | | $h'(0)$ | | A | |
|-------|----------|----------|---------|---------|----------|----------|
| | Ref. 31 | present | Ref. 31 | present | Ref. 31 | present |
| 0.1 | -0.96938 | -0.96939 | 0.26278 | 0.26338 | 0.79170 | 0.79170 |
| 0.3 | -0.84942 | -0.84942 | 0.60573 | 0.60633 | 0.51949 | 0.51950 |
| 0.8 | -0.29938 | -0.29939 | 0.93430 | 0.93473 | 0.11452 | 0.11453 |
| 1 | 0 0 | 1 | 1 | 0 | 0 | |
| 2 | 2.01750 | 2.01749 | 1.16489 | 1.16521 | -0.41040 | -0.41041 |
| 3 | 4.72928 | 4.72924 | 1.23438 | 1.23464 | -0.69305 | -0.69305 |
| 4 | 8.00042 | 8.00036 | 1.27272 | 1.27300 | -0.91650 | -0.91650 |

- (ii) The domain $[0, y_\infty]$ is divided into n subintervals $[0, y_1], [y_1, y_2], [y_2, y_3] \dots [y_{n-1}, y_n = y_\infty]$. For convergence of solution, n can be increased sufficiently.
- (iii) The problem is solved over each subinterval such that it satisfies the boundary conditions at y_∞ .
- (iv) Initial guess is supplied for the first interval and then the obtained solution is taken as initial guess for the next interval and so on.
- (v) Algorithm is developed in MATLAB R2010a.

4. Results and discussion

The nonlinear ordinary differential Eqs. (30), (32), and (34) with boundary conditions (33) and (35) have been solved numerically. The numerical values of $f''(0)$, $h'(0)$, A and Nusselt number are shown in tables. In Table I, the comparison is given for $f''(0)$, $h'(0)$, and boundary layer displacement ‘ A ’ with results obtained by Labropulu *et al.* [32] when $\beta = 0$. It is found that the calculated results are highly accurate and in good agreement with Labropulu [32]. It can be seen from

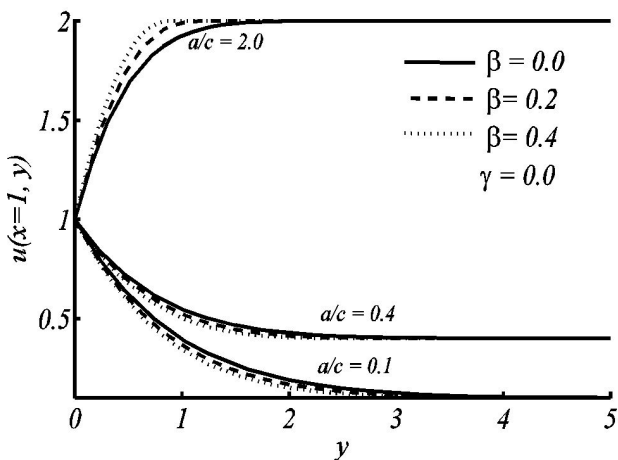


FIGURE 2. Variation in horizontal velocity profile u along y for the different values of β , when $a/c = 0.1, 0.4, 2.0$ and $\gamma = 0$.

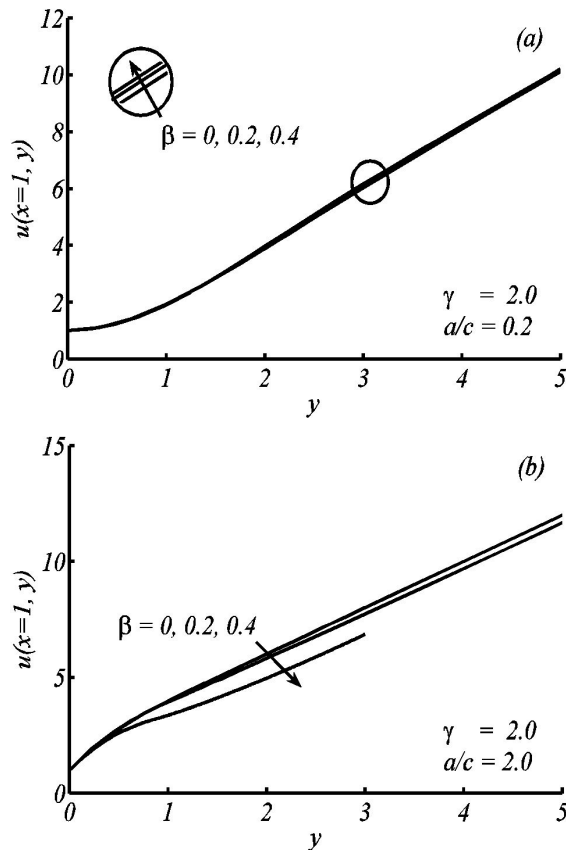


FIGURE 3. Variation in horizontal velocity profile u along y , for the different values of β , when (a) $a/c = 0.2$, (b) $a/c = 2.0$ and $\gamma = 2.0$ are fixed.

the Table I that the value of $f''(0)$ is increasing with the increase of a/c . The comparison of Nusselt number with the result obtained by Pop *et al.* [31] is shown in Table II. The results shown in braces are reported by Pop *et al.* [31]. Present results as a limiting case are shown in the Tables I and II, which establish a good agreement with the previous results. However, a small difference arises due to change in numerical technique. In present study the parallel shooting method is used where Pop *et al.* [31] solved with the help of simple shooting method. For infinite domain, simple

TABLE II. The Numerical values of Nusselt number for the different values of β , a/c and Pr.

| a/c | Pr | Newtonian fluid ($\beta = 0$) | | | | Maxwell fluid ($\beta = 0.2$) | | | |
|-----|----------|---------------------------------|----------|----------------|----------|---------------------------------|---------|----------------|----------|
| | | $\theta_w = 1.1$ | | $\theta_w = 2$ | | $\theta_w = 1.1$ | | $\theta_w = 2$ | |
| | | Rd=1 | Rd=10 | Rd=1 | Rd=10 | Rd=1 | Rd=10 | Rd=1 | Rd=10 |
| 0.1 | 0.05 | 0.11617 | 0.25815 | 0.17507 | 0.47034 | 0.11395 | 0.25587 | 0.17287 | 0.46827 |
| | | (0.1159) | (0.2587) | (0.1750) | (0.4737) | | | | |
| | 0.5 | 0.52056 | 0.98655 | 0.72129 | 1.64850 | 0.50358 | 0.96460 | 0.69977 | 1.62669 |
| | | (0.5194) | (0.9861) | (0.7210) | (1.6473) | | | | |
| 0.5 | 1.0 | 0.83618 | 1.53603 | 1.15670 | 2.47460 | 0.81017 | 1.49404 | 1.11685 | 2.43044 |
| | | (0.8337) | (1.5335) | (1.1550) | (2.4763) | | | | |
| | 1.5 | 1.09838 | 2.00807 | 1.53495 | 3.16612 | 1.06728 | 1.94792 | 1.48047 | 3.09981 |
| | | (1.0946) | (2.0040) | (1.5318) | (3.1654) | | | | |
| 1.0 | 0.05 | 0.21346 | 0.53127 | 0.34720 | 1.00664 | 0.21240 | 0.53059 | 0.34608 | 1.00489 |
| | | (0.2131) | (0.5305) | (0.3465) | (1.0013) | | | | |
| | 0.5 | 0.72884 | 1.74413 | 1.15842 | 3.246117 | 0.72128 | 1.73363 | 1.14868 | 3.23508 |
| | | (0.7267) | (1.7461) | (1.1573) | (3.2408) | | | | |
| 2.0 | 1.0 | 1.06582 | 2.51678 | 1.68455 | 4.64451 | 1.05397 | 2.49782 | 1.66709 | 4.62336 |
| | | (1.0621) | (2.5121) | (1.6823) | (4.6404) | | | | |
| | 1.5 | 1.33262 | 3.12665 | 2.10291 | 5.73795 | 1.31792 | 3.09850 | 2.07912 | 5.70632 |
| | | (1.3268) | (3.1194) | (2.0988) | (5.7386) | | | | |
| 1.0 | 0.05 | 0.28805 | 0.73736 | 0.47746 | 1.40927 | 0.28805 | 0.73736 | 0.47746 | 1.40927 |
| | | (0.2888) | (0.7517) | (0.4772) | (1.4104) | | | | |
| | 0.5 | 0.91092 | 2.33066 | 1.50985 | 4.45631 | 0.91092 | 2.33066 | 1.50985 | 4.45631 |
| | | (0.9081) | (2.3283) | (1.5085) | (4.4574) | | | | (4.4574) |
| 1.0 | 1.0 | 1.28824 | 3.29605 | 2.13525 | 6.30218 | 1.28824 | 3.29605 | 2.13525 | 6.30218 |
| | | (1.2833) | (3.2882) | (2.1315) | (6.2985) | | | | |
| | 1.5 | 1.57778 | 4.03682 | 2.61515 | 7.71856 | 1.57778 | 4.03682 | 2.61515 | 7.71856 |
| | | (1.5699) | (4.0268) | (2.6098) | (7.7089) | | | | |
| 2.0 | 0.05 | 0.39551 | 1.02982 | 0.66345 | 1.98097 | 0.39506 | 1.01129 | 0.65865 | 1.90525 |
| | | (0.3948) | (1.0292) | (0.6627) | (1.9811) | | | | |
| | 0.5 | 1.18876 | 3.17994 | 2.02722 | 6.18570 | 1.20143 | 3.18483 | 2.04074 | 6.14863 |
| | | (1.1842) | (3.1738) | (2.0242) | (6.1801) | | | | |
| 1.0 | 1.64141 | 4.43873 | 2.81466 | 8.68359 | 1.66308 | 4.46166 | 2.84334 | 8.67191 | |
| | (1.6332) | (4.4280) | (2.8093) | (8.6779) | | | | | |
| 1.5 | 1.97902 | 5.38551 | 3.39844 | 10.57659 | 2.00662 | 5.42352 | 3.44386 | 10.58412 | |
| | (1.9675) | (5.3690) | (3.3938) | (10.5729) | | | | | |

shooting method is hard to use due to its dependence on initial guess. In present study, the boundary edge reaches to $y = 200$, for large value of radiation parameter and small Prandtl number. It is observed from the Table II, with the increase of radiation parameter Rd the Nusselt number increases *i.e.* heat transfer rate increases with Pr, a/c and keeping θ_w fixed. It is further observed that the value of Nusselt number increases with increase of Prandtl number (Pr) due to reason that the Prandtl number is directly proportional to the

viscosity of the fluid. Increase in Prandtl number, physically means viscosity of the fluid increases.

The effects of parameters namely, the velocity ratio parameter a/c , the Deborah number β , the shearing parameter γ , the radiation parameter Rd, and the surface heating parameter θ_w on the velocity and temperature profiles are shown through Figs. 2-8. In Fig. 2, it is seen that due to stretching and straining velocities two boundary layer structures appear as reported by Mahapatra and Gupta [27]. Figures 2 and 3

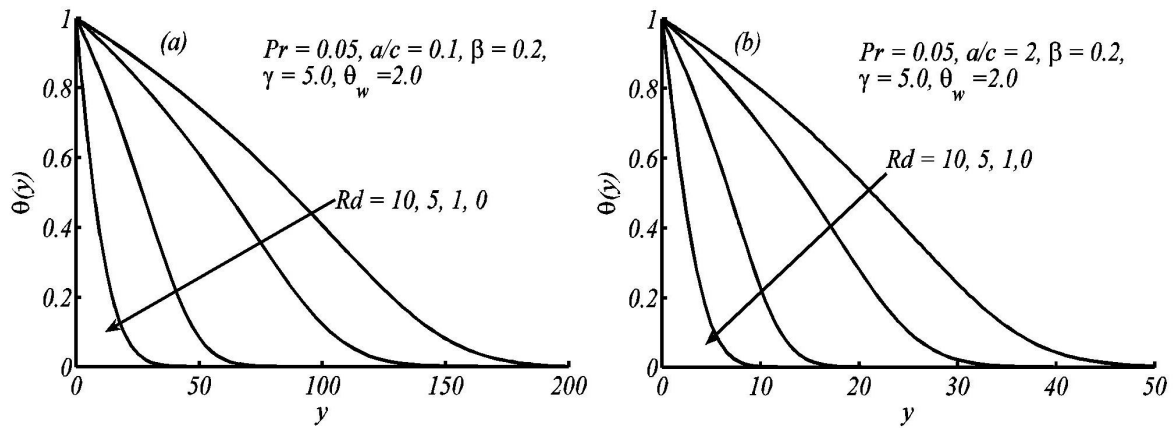


FIGURE 4. Variation in temperature profile $\theta(y)$ for the different values of Rd , when $Pr = 0.05$, $\beta = 0.2$, $\gamma = 5.0$, and $\theta_w = 2.0$ are fixed.

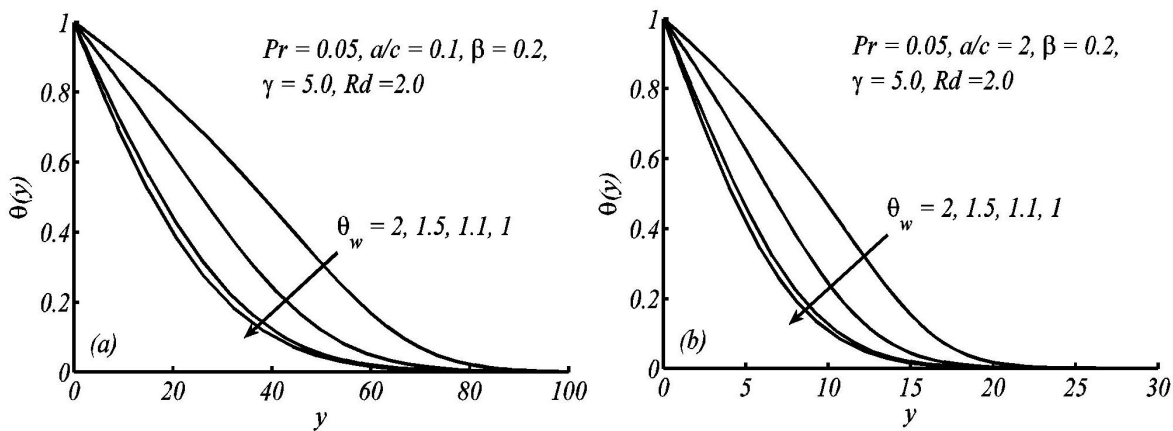


FIGURE 5. Variation in temperature profile $\theta(y)$ for the different values of θ_w , when $Pr = 0.05$, $\beta = 0.2$, $\gamma = 5.0$, and $Rd = 2.0$ are fixed.

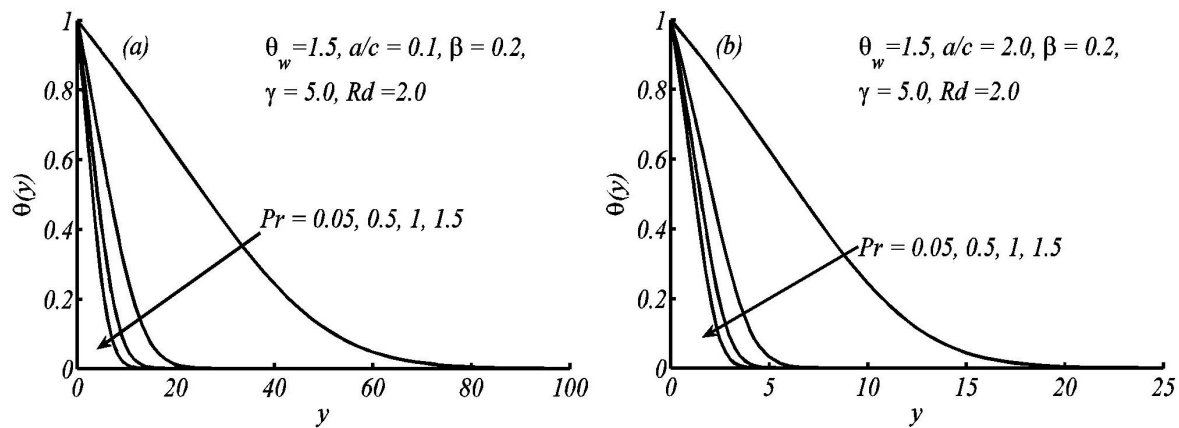


FIGURE 6. Variation in temperature profile $\theta(y)$ for the different values of Pr , when $\theta_w = 1.5$, $\beta = 0.2$, $\gamma = 5.0$, and $Rd = 2.0$ are fixed.

depict the behavior of orthogonal stagnation point flow and oblique stagnation point flow ($\gamma = 0$) respectively for the different values of β . From Fig. 2, It is observed that for $a/c < 1$ boundary layer thickness and velocity decrease with the increase in values of β but for $a/c > 1$ velocity increases and the boundary layer thickness decreases, with the increase

in values of β . In Fig. 3(a), it is observed that the effect of β is very small for small values of a/c . It is noticed that the velocity of the fluid increases with the increase of when $a/c < 1$ and it decreases with the increase in β when $a/c > 1$.

Figure 3 illustrates that the velocity in the case of non-orthogonal stagnation point flow is greater than that of or-

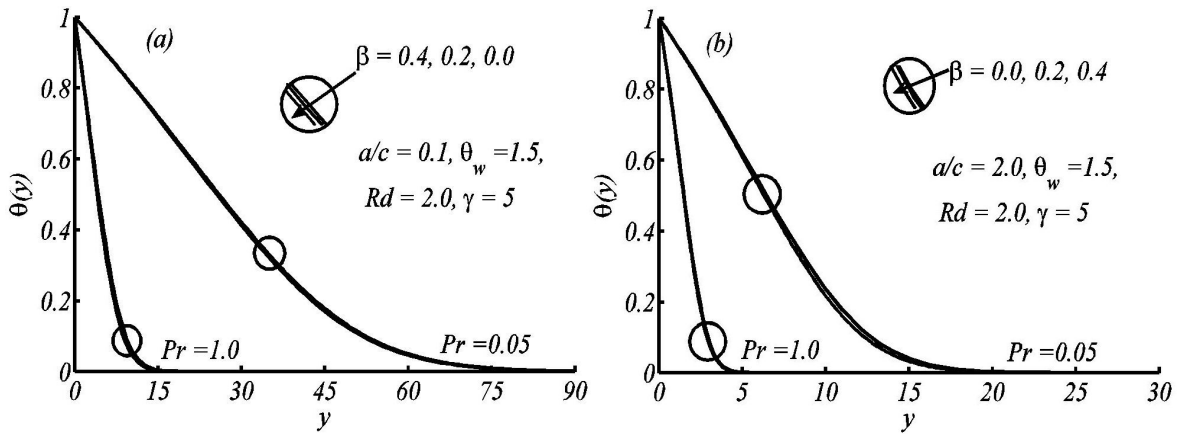


FIGURE 7. Variation in temperature profile $\theta(y)$ for the different values of a/c , when $Pr = 0.05$, $\beta = 0.2$, $\gamma = 5.0$, and $\theta_w = Rd = 2.0$ are fixed.

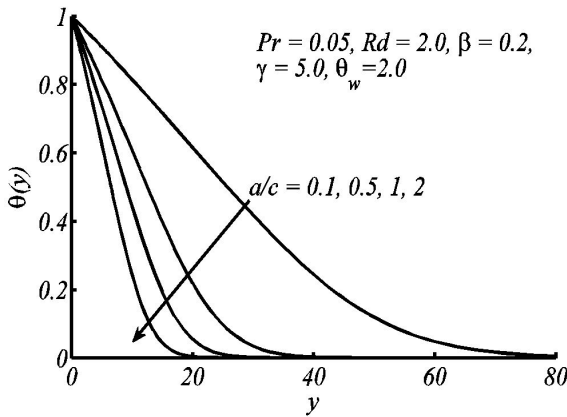


FIGURE 8. Variation in temperature profile $\theta(y)$ for the different values of a/c , when $Pr = 0.05$, $\beta = 0.2$, $\gamma = 5.0$, and $\theta_w = Rd = 2.0$ are fixed.

thogonal stagnation point flow. Figures 4 and 5 show the temperature profiles for the different values of the radiation-conduction parameter Rd and surface heating parameter respectively. In both figures, the thermal boundary layer thickness increases with the increase of radiation-conduction parameter and surface heating parameter. Figure 6 shows the effects of Prandtl number on the temperature profile for small and large values of a/c . It depicts that with the increase of Prandtl number, the thermal boundary layer thickness decreases, meaning that fluids of high Prandtl number are responsible for more heat transfer. The effects of Deborah number β on temperature profile have also been shown in Fig. 7(a,b) for both small and large values of Prandtl number. Figure 7(a) shows the temperature profile for $a/c = 0.1$. In this case thermal boundary thickness increases with increase in the values of β . On the other hand, Fig. 7(b) shows an opposite behavior *i.e* thermal boundary thickness decreases with increase in the values of β . In Fig. 8, the temperature profile for the different values of a/c (ratio of straining and stretching) is shown which depicts that with increase of a/c , thermal boundary layer thickness decreases respectively.

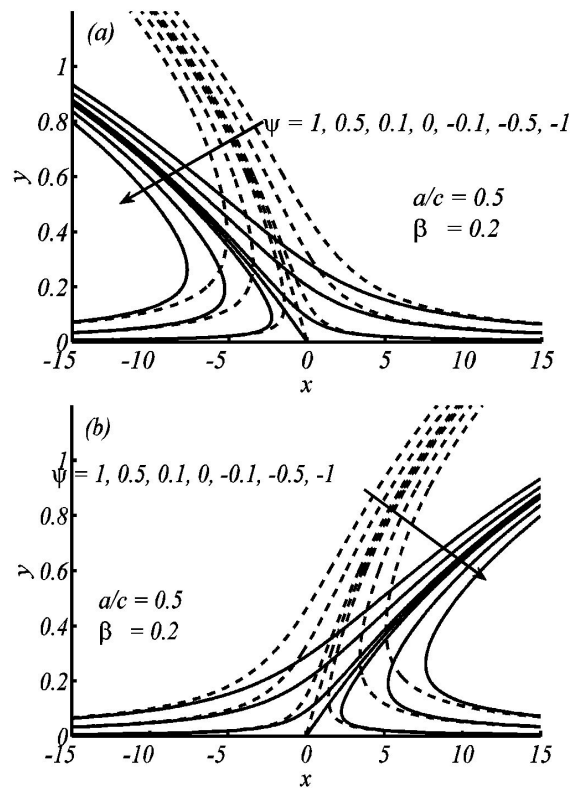


FIGURE 9. Streamlines for oblique flow (a) $\gamma = 10$ (*dashedlines*), $\gamma = 30$ (*solidlines*) (b) $\gamma = -10$ (*dashedlines*) $\gamma = -30$ (*solidlines*). when $\beta = 0.2$, $a/c = 0.5$ are fixed.

Figures 9 and 10 show the flow pattern of the oblique stagnation point flows ($\gamma \neq 0$). Both cases of favorable ($\gamma > 0$) and unfavorable ($\gamma < 0$) are considered. Figure 9 illustrates the increase in obliqueness with increase in the values of shearing parameter γ . In the stagnation point region the velocity of the fluid increases with increase in the values of $|\gamma|$. Figure 10 further shows that by increasing free stream velocity, the streamlines of oblique stagnation point flow look like those of the orthogonal stagnation point flow.

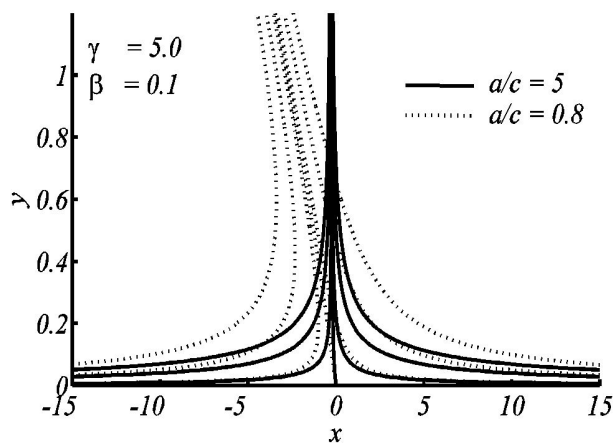


FIGURE 10. Stream lines for oblique flow, when $\beta = 0.1$ and $\gamma = 5$ for the different values of a/c .

5. Concluding remarks

The radiation effects on the flow of Maxwell fluid near the oblique stagnation point over a stretching sheet is studied. The effects of different parameters on heat and fluid flow are discussed through graphs and tables. This study concludes that the boundary layer thickness decreases with increase of a/c in the oblique stagnation point flow. The thermal boundary layer thickness increases with the increase of radiation-conduction and surface heating parameters. It is also noted that with the increase of free stream velocity the temperature of the fluid decreases near the wall. On the other hand, temperature of the fluid increases with increase of stretching velocity. The velocity of the fluid also increases with the increase of shearing parameter γ .

1. G.I. Burde, *ASME J. of Fluids Engineering* **117** (1995) 189-191.
2. H. Ujiie, D.W. Liepsch, M. Goetz, R. Yamaguchi, H. Yonetani, and K. Takakura, *Stroke* **27** (1996) 2086-94.
3. E. Magyari, and B. Keller, *Eur. J. Mech. B Fluids* **19** (2000) 109-122.
4. J.E. Higham, W. Brevis, C.J. Keylock and A. Safarzadeh, *Advances in Water Resources* **107** (2017) 451-459.
5. J.T. Stuart, *J. Aerospace Sci.* **26** (1959) 124-125.
6. K.J. Tamada, *J. Physical Soc. Jpn.* **47** (1979) 310-311.
7. J.M. Dorrepaal, *J. Fluid Mech.* **163** (1986) 141-147.
8. M. Reza and A.S. Gupta, *Fluid Dynamic Research* **37** (2005) 334-340.
9. I. Husain, F. Labropulu and I. Pop, *Central Eur. J. Phys.* **9** (2011) 176-182.
10. T.R. Mahapatra, S.K. Nandy and A.S. Gupta, *Meccanica* **47** (2012) 1325-1335.
11. Y.Y. Lok, I. Pop and D.B. Ingham, *Mechanica* **45** (2010) 187-198.
12. L.V. Yajun and Z. Liancun, *Int. J. Eng. Sci. Innovative Tech.* **2** (2013) 200-209.
13. S. Wang and W.C. Tan, *Int. J. Heat Fluid Flow*, **32** (2011) 88-94.
14. N.F.M. Noor, *World Acad. Sci. Eng. Technol.* **64** (2012).
15. T. Javed and A. Ghaffari, *Journal of Mechanics* **32** (2016) 175-184.
16. M.S. Abel, V. Tawade and N. Shinde, *Adv. Math. Phys.* (2012) 702681.
17. S. Mukhopadhyaya, *Chin. Phys. Lett.* **29** (2012) 054703.
18. S. Nadeem, Rizwan Ul Haq, and Z.H. Khan, *Journal of the Taiwan Institute of Chemical Engineers* **45** (2014) 121-126.
19. E. Magyari and B. Keller, *Eur. J. Mech. B Fluids* **19** (2000) 109-122.
20. L.J. Crane, *Z Angew Math. Phys.* **21** (1970) 645-647.
21. K.R. Rajagopal, T.Y. Na and A.S. Gupta, *Rheol. Acta* **23** (1984) 213-215.
22. T.R. Mahapatra and A.S. Gupta, *Acta Mech.* **152** (2001) 191-196.
23. R. Nazar, N. Amin, D. Filip and I. Pop, *Int. J. Nonlinear Mech.* **39** (2004) 1227-1235.
24. G.C. Layek, S. Mukhopadhyay and S.K.A. Samad, *Heat Mass Transfer*, **34** (2007) 347-356.
25. T. Hayat, T. Javed and Z. Abbas, *Nonlinear Anal. Real World Appl.* **10** (2009) 1514-1526.
26. J. Zhu, L. Zheng and Z.G. Zhang, *Appl. Math. Mech.* **31** (2010) 439-48.
27. K. Bhattacharyya, *Ain Shams Eng. J.* **4** (2013) 259-264.
28. P.S. Gupta and A.S. Gupta, *Can. J. Chem. Eng.* **55** (1977) 744-746.
29. T.R. Mahapatra and A.S. Gupta, *Heat Mass Transfer*, **38** (2002) 517-21.
30. A. Raptis, C. Perdikis and H.S. Takhar, *Appl. Math. Comput.* **153** (2004) 645-649.
31. S. R. Pop, T. Grosan and I. Pop, *Techn. Mech.* **25** (2004) 100-106.
32. F. Labropulu, D. Li and I. Pop, *Int. J. Thermal Sci.* **49** (2010) 1042-1050.
33. M. Sajid, Z. Abbas, T. Javed and N. Ali, *Can. J. Phy.* **88** (2010) 635-640.
34. T. Cebeci and H.B. Keller, *J. Comput. Phys.* **7** (1971) 289-300.